

Collective variable theory for optical solitons in fibers

P. Tchofo Dinda, A. B. Moubissi, and K. Nakkeeran

Laboratoire de Physique de l'Université de Bourgogne, UMR CNRS No. 5027, avenue A. Savary, Boîte Postale 47 870, 21078 Dijon Cédex, France

(Received 29 December 2000; revised manuscript received 27 February 2001; published 22 June 2001)

We present a projection-operator method to express the generalized nonlinear Schrödinger equation for pulse propagation in optical fibers, in terms of the pulse parameters, called collective variables, such as the pulse width, amplitude, chirp, and frequency. The collective variable (CV) equations of motion are derived by imposing a set of constraints on the CVs to minimize the soliton dressing during its propagation. The lowest-order approximation of this CV approach is shown to be equivalent to the variational Lagrangian method. Finally, we demonstrate the application of this CV theory for pulse propagation in dispersion-managed optical fiber links.

DOI: 10.1103/PhysRevE.64.016608

PACS number(s): 42.81.Dp, 42.65.Tg

I. INTRODUCTION

The propagation of intense light pulses in a standard telecommunication fiber can induce a host of nonlinear phenomena, such as parametric wave mixing, stimulated Raman scattering, or self-steepening, to name a few [1,2]. The combined effects of nonlinear phenomena and the fiber chromatic dispersion lead to many interesting dynamical processes which are difficult to understand in terms of the original pulse field, but can be easily understood by applying a collective variable (CV) approach. For example, the dynamics of the propagation of light pulses in an optical fiber can be completely described by a field, say ψ , which is a solution of certain nonlinear partial differential equation commonly referred as “generalized nonlinear Schrödinger equation” (NLSE). Exact expression of ψ may be given by a complicated form, depending on the type of dispersive and (or) nonlinear effects appearing in the evolution equation of the fiber [1,2]. Usually, it is difficult to ascertain directly from the original field ψ what is exactly happening during the pulse propagation. Hence, the field ψ , which describes the dynamics of the pulse and other excitations of the system such as radiations, must be analyzed with extreme care to follow exactly the pulse trajectories in the phase space. The pulse dynamics will become even more complicated in the case of systems that are not integrable. For instance, in optical communications, it was shown that pulses propagating in dispersion-managed (DM) fiber links, called “DM solitons,” possess a richer temporal and spectral structure of modes than a simple collective entity [3]. That is, a DM soliton is not only able to translate like a whole entity, but can also vibrate like a diatomic molecule [3]. Hence, it is useful, especially in such nonintegrable systems, to associate new variables, called collective variables, with localized collective phenomena, in order to simplify somehow the description of the pulse dynamics. For example, such CVs may represent the amplitude of a pulse, its temporal position, the pulse width, and so on. The number of CVs that can be introduced into the system is usually determined by the physics under consideration. Then one must derive a transformation which allows us to express the original field equation in terms of CVs. In other words, one must derive the equations

of motion for the CVs, whose solutions will explicitly yield the complete dynamics of the nonlinear localized modes under consideration.

Such CV theories have been successfully applied to condensed matter systems, in particular to nonlinear Klein-Gordon and similar systems [4–11]. Various approaches such as Lagrange dynamics with Lagrange multipliers [5], Hamiltonian dynamics using Dirac brackets [12], and projection-operator methods [6–11,13,14] have been used to derive the CV equations of motion. In particular, one of the most useful results of CV theory in the condensed matter systems was obtained by Boesch *et al.* [6]. They developed a projection-operator formalism which makes the derivation of the CV equations of motion very simple [6]. They used this formalism to derive the exact equations of motion for the center of mass of a discrete sine-Gordon kink and the frequency of its small oscillations in the Peierls-Nabarro well [7]. The projection-operator approach was also used to calculate the spontaneous emission of radiation from a discrete sine-Gordon kink [8], the effects of lattice discreteness on the statistical mechanics of a dilute gas of kinks [9], and the dynamics of the discrete sine-Gordon breather [13]. This approach has also been successful in treating the effects of lattice discreteness in many other nonlinear Klein-Gordon systems which support stable kink structures such as the double-quadratic kink [10], or the double-sine Gordon kink [11].

Quite in contrast, the actual stage of CV treatments of nonlinear partial differential equations in nonlinear fiber optics happens to be surprisingly much less elaborated than in condensed matter physics. One of the reasons for this is that, from the period of invention of optical solitons up to very recent years, the main line of research in ultrahigh capacity fiber communications was based on the concept of the “classical soliton,” which represents an exact balance between the fiber group-velocity dispersion and its intensity-dependent refractive index. This soliton arises as a solution for the standard NLSE, with a well-known hyperbolic secant profile that can be obtained by different techniques (e.g., the inverse scattering transform [15]), without going through any CV approach [16]. However, well before the first experimental observation of solitons in optical fibers in 1980 [17], it

has been predicted that electromagnetic waves propagating in nonlinear dielectric media may become unstable in the presence of various perturbing effects (e.g., noise, loss, cross interactions) [18,19]. Quite naturally, in most of the early literature which have used CVs in the context of optical solitons in fibers, a significant effort was made to analyze the soliton dynamics under the influence of such perturbing factors [20–26]. Different perturbation theories were developed, using the adiabatic variation of conserved quantities of the NLSE [20], the adiabatic variation of the scattering data based on the inverse scattering transform [21,22], or the Lagrangian perturbation theory [24]. Kath and Smyth employed a trial function which consists of a solitonlike pulse with variable parameters plus a linear dispersive term in an averaged Lagrangian to study the dispersive radiative losses for the NLSE [27]. But these perturbation theories yield consistent results only in the limit of weak perturbations. This limitation has led to the formulation of nonperturbative CV theories for the NLSE using the averaged Lagrangian method [3,28–36]. Most of the recent and current theoretical developments have employed this Lagrangian method to describe pulse propagation in DM fiber links [37–40]. A major line of current research focuses on the modelization of soliton transmission in DM fiber-optic links, with a view both to upgrade the capacity of existing terrestrial networks and to design submarine fiber systems [3,41]. Basically, the dispersion-management technique utilizes a transmission line with a periodic dispersion map, such that each period is built up by two types of fiber, generally with different lengths and opposite ground-velocity dispersion. The main limitations to the transmission capacity of such systems include various effects such as the cross-phase modulation, filtering, phase and amplitude modulation, third-order dispersion, stimulated Raman scattering, and self-steepening.

However, most of the above-mentioned CV theories for optical solitons in fibers [3,20–36] have a common feature that the soliton dressing is completely ignored, which can lead to dramatic consequences depending on the choice of the ansatz function. In condensed matter physics, approximation of neglecting the soliton dressing is called ‘‘bare approximation.’’ Generally, this approximation leads to a simple set of ordinary differential equations that describe the evolution of the CVs, with different degrees of accuracy depending on the choice of the ansatz function. However, the bare approximation yields consistent results only when there is no considerable radiation and the dressing is also negligible. This is remarkably well illustrated in a recent study by Abdullaev and Caputo [42], who performed a careful analysis of the validity of the bare approximation for a single-pulse propagation in a system with spatially varying dispersion. In particular they showed that the bare approximation yields very poor results in all the situations where the radiation field is important [42]. The main reason for which the dressing has been largely neglected so far lies in the high degree of complexity of the CV treatment of the generalized NLSE, in which the fiber parameters become functions of the propagation distance in the case of DM systems. The approximate treatment of the generalized NLSE leads to a class of challenging and interesting problems related to higher-

order effects such as stimulated Raman scattering, third-order dispersion, self-steepening, and their combined effects in DM fiber lines, which have not yet been sufficiently understood theoretically. A useful step towards a best understanding of those problems lies in the development of a complete CV theory for optical solitons in fibers that carefully takes into account the soliton dressing.

In this paper, we present a rigorous CV treatment of the generalized NLSE for optical solitons in fibers. In this CV theory, we use a projection-operator formalism, in a similar way to that developed by Boesch *et al.* [6] for the CV treatment of the nonlinear Klein-Gordon kink equation in condensed matter physics. But there exists a major difference between these two types of equations in their degree of complexity. From the Lagrangian corresponding to the nonlinear Klein-Gordon kink equation one can straightforwardly derive the canonical transformation of this equation into the CV equations of motion, whereas there is no Lagrangian available for the generalized NLSE. In the present paper, although we do not derive the canonical transformation, we describe the essential steps to express the generalized NLSE in terms of CV equations of motion. Furthermore, our CV approach is complete in the sense that we have the equations of motion not only for the CVs but also for the residual field, which includes the soliton dressing and any radiation coupled to the soliton’s motion. In Ref. [43], we have presented a CV treatment for DM fiber links. That letter gives the basic idea of the CV theory for the generalized NLSE [43]. One of the most useful advantages of our present CV approach for the generalized NLSE is its equivalence to a projection-operator formalism, which makes the derivation of the CV equations of motion relatively simple. Another important feature in this paper is the direct residual-field minimization, which is a fully numerical procedure for quickly applying this CV theory.

The paper is organized as follows. In Sec. II, we present the CV theory for the generalized NLSE, using the projection-operator scheme. In Sec. III, we describe a simple and practical numerical procedure, which is strictly equivalent to complete CV theory, that allows us to obtain the evolution of the CVs directly from the generalized NLSE immediately, i.e., without any need to solve the entire CV equations. We demonstrate the application of this CV theory for the propagation of optical pulses in a typical DM optical fiber transmission lines in Sec. IV. Finally, in Sec. V we conclude.

II. COLLECTIVE VARIABLE THEORY

Nonlinear pulse propagation in fiber links may be described by the generalized NLSE [1,2]:

$$\begin{aligned} \psi_z + i \frac{\beta_2(z)}{2} \psi_{tt} - i \gamma(z) |\psi|^2 \psi \\ = - \frac{\alpha(z)}{2} \psi + \frac{\beta_3(z)}{6} \psi_{ttt} - i \gamma_r(z) \psi (|\psi|^2)_t \\ - \gamma_s(z) (|\psi|^2 \psi)_t, \end{aligned} \quad (1)$$

where $\psi(z,t)$ is the envelope amplitude of the electric field measured in units of square root of Watts at position z in the fiber and at time t , the subscript z (or t) on ψ denotes the partial derivative with respect to z (or t). The parameters $\beta_2(z)$ and $\beta_3(z)$ represent the second- and third-order dispersion coefficients, respectively. The parameter $\gamma(z) \equiv [n_2(z)\omega_0]/[c A_{\text{eff}}(z)]$ measures the strength of the nonlinearity, c denotes the speed of light, $n_2(z)$ is the nonlinear index coefficient, $A_{\text{eff}}(z)$ is the effective core area, and ω_0 is the frequency of the carrier wave. $\alpha(z)$ represents the linear loss in the fiber, $\gamma_r(z) \equiv \gamma(z)T_R$ represents the Raman gain, T_R measures the slope of the Raman gain curve for small frequency detunings from ω_0 . The parameter $\gamma_s(z) \equiv 2\gamma(z)/\omega_0$ represents the self-steepening coefficient.

It is important to note that some parameters appearing in the above-generalized NLSE may need to be slightly modified to precisely describe the pulse propagation in some specific situations. For example, for a DM fiber links, the coefficient $\beta_2(z)$ [and even $\alpha(z)$, $\beta_3(z)$, and $\gamma(z)$] will vary periodically along the propagation distance. More generally, the most important point to be emphasized here is that our CV approach is formulated in a way such that if any of the coefficients in the generalized NLSE (1) is modified, then the same modification has to be carried out straightaway in the final CV equations of motion.

The idea in CV theory is to associate new variables (collective variables) with the quantities of interest for which equations of motion can be derived, whose solutions yield explicitly the dynamics of the nonlinear localized modes under consideration. That is, one may introduce N CVs, symbolically X_j ($j=1, \dots, N$), which are associated with the nonlinear localized modes (soliton's width, amplitude, frequency, and so on). To this end, we decompose the original field in the following way:

$$\psi(z,t) = f(X_1, X_2, \dots, X_N, t) + q(z,t), \quad (2)$$

where the ansatz function f is chosen to be the best representation of the configuration of the pulse and $q(z,t)$ is the remaining field such that the sum of f and q satisfy the original generalized NLSE (1). Note that the most commonly chosen ansatz function for optical solitons in fiber is a Gaussian profile [1–3]. One can also choose any other suitable profile for f . For example, f can be a hyperbolic secant profile [25], or an expansion in terms of Hermite-Gaussian polynomials [44–46]. In all cases, the field q , that we call *residual field*, will account for the dressing of the pulse and any radiation coupled to the pulse's motion. One cannot simply substitute $\psi = f + q$ into the generalized NLSE (1) because the introduction of the CVs in f (as dynamical variables) will give extra degrees of freedom into the system, which can enlarge the available phase space of the system [6,47]. Simply substituting ψ into Eq. (1) would therefore introduce new and undesirable solutions into the system [6,47]. One must constrain the system of new variables (i.e., CVs and q) so that the system remains in the same phase space as the original field equation (1). The first set of constraints is obtained by configuring the ansatz function f to be the best fit to the field ψ . In other words, the CVs

X_1, X_2, \dots, X_N are obtained by configuring that the ansatz function $f(X_1, X_2, \dots, X_N)$, minimizes the functional Λ , where

$$\Lambda \equiv \int_{-\infty}^{\infty} |q|^2 dt = \int_{-\infty}^{\infty} |\psi - f(X_1, X_2, \dots, X_N, t)|^2 dt. \quad (3)$$

In this CV approach, the quantity Λ , corresponding to the total amount of the energy in the residual field, serves as a measure for the correctness of the ansatz function f . A fundamental point, neglected in previous CV treatments of optical solitons in fibers, is that the residual field energy (RFE) Λ must be sufficiently small to give proper physical meaning for the CVs. The constraints that we impose on the system will allow the CVs to evolve only in a particular direction to minimize the RFE during the dynamics, in the following simple way:

$$C_j = \frac{d\Lambda}{dX_j} \approx 0. \quad (4)$$

Equations (4), (3), and (2) lead to the following constraint conditions

$$C_j = \int_{-\infty}^{\infty} \text{Re} \left[q \frac{\partial f^*}{\partial X_j} \right] dt \approx 0, \quad (5)$$

where Re denotes real part. In Eqs. (4) and (5), the sign “ \approx ” indicates the Dirac's weak equality [12]. Indeed, our procedure for obtaining the equations of motion for the CVs and coupled field q is based on the Dirac theory of constrained dynamical systems [12]. In Dirac's terminology, a quantity which is weakly equal to zero cannot be set to zero until all variations of the quantity with respect to the dynamical variables, to obtain the equations of motion, have been performed [12]. A careful analysis of the proper way of incorporating such constraints in CV theories is carried out in Ref. [14]. In this context, a fundamental point to be emphasized is that the initial values of the CVs, $X_j(z=0)$, must be chosen to satisfy the constraint conditions. The constraints which are satisfied at the beginning of the dynamics (i.e., at $z=0$) do not guarantee that they will be satisfied throughout the propagation distance z . Consequently, we must introduce a second set of constraints, which will guarantee that the first set of constraints C_j will be satisfied for all z if they are initially satisfied, i.e., $C_j(X_1, X_2, \dots, X_N, z=0) \approx 0$. Thus, we define the second set of constraints as

$$\frac{dC_j}{dz} \approx 0. \quad (6)$$

Substitution of Eq. (2) into the generalized NLSE (1) directly yields the equation of motion for the residual field:

$$\begin{aligned}
& q_z + i \frac{\beta_2(z)}{2} q_{tt} - \frac{\beta_3(z)}{6} q_{ttt} - i \gamma(z) |f+q|^2 q + \frac{\alpha(z)}{2} q \\
& + i \gamma_r(z) (|f+q|^2)_t q + \gamma_s(z) (|f+q|^2)_t q_t \\
& = - \sum_{j=1}^N \dot{X}_j f_{X_j} - i \frac{\beta_2(z)}{2} f_{tt} + \frac{\beta_3(z)}{6} f_{ttt} + i \gamma(z) |f+q|^2 f \\
& - \frac{\alpha(z)}{2} f - i \gamma_r(z) (|f+q|^2)_t f - \gamma_s(z) (|f+q|^2)_t f_t,
\end{aligned} \tag{7}$$

where the overhead dot represents the derivative with respect to z and the subscript X_j on f denotes the partial derivative with respect to X_j . To obtain the CV equations of motion, we project Eq. (7) in the direction of

$$\mathcal{P}_k = \frac{\partial f^*}{\partial X_k}. \tag{8}$$

That is, multiplying Eq. (7) by \mathcal{P}_k and integrating the real part of the resulting equation with respect to t , gives

$$[\dot{X}] = - \left[\frac{\partial C}{\partial X} \right]^{-1} [\mathcal{R}], \tag{9}$$

which coincides exactly with Eq. (12) of Ref. [43]. In the above Eq. (9), $[X]$, $[C]$, and $[\mathcal{R}]$ are column vectors of X_j , C_j , and elements involving α , β_2 , γ , β_3 , γ_r , and γ_s , given explicitly in Ref. [43]. The set of Eqs. (7) and (9) represents the complete CV treatment for the generalized NLSE (1).

The lowest-order approximation of the CV theory, called ‘‘bare approximation,’’ is obtained by setting the residual field to zero [$q(z,t)=0$]. In this case one can assume the desired form for the ansatz function f . In Ref. [43], we have assumed a Gaussian ansatz function and explicitly derived the bare CV equations. When optical losses and all the higher-order terms of the generalized NLSE (1) are considered as perturbation terms, then it is possible to make use of the perturbed Lagrangian method to derive the CV equations of motion, as we show in Appendix A. The equations obtained by the perturbed Lagrangian method coincide exactly with the bare CV equations derived using our CV theory. Therefore, the perturbed Lagrangian approach corresponds to the lowest-order approximation of the complete CV theory which explicitly includes the soliton dressing and any radiation coupled to the soliton’s motion.

III. DIRECT RESIDUAL-FIELD MINIMIZATION

In this section, we present a simple and fully numerical procedure, which is strictly equivalent to the resolution of the above equations of motion (7) and (9), and which requires only a very small fraction of calculations for obtaining the motion of the CVs and the residual field. This procedure, which lies in the direct minimization of the RFE [Eq. (3)], requires to solve numerically the generalized NLSE (1) for the original field $\psi(z,t)$ (e.g., by use of the split-step Fourier

transform method [1]). Then, at each propagation distance z , the first set of constraint conditions (5) is used to obtain the set of CVs which minimizes the RFE. Note that when the field $\psi(z,t)$ is known at a given distance z , then solving the set of Eq. (5) becomes the familiar problem of minimization of a functional with respect to N variables (CVs). This problem can be solved by means of the following iterative procedure, which corresponds to the Newton-Raphson method of minimization procedure [48]:

$$[X]_{i+1} = [X]_i - \left[\frac{\partial C}{\partial X} \right]_i^{-1} [C]_i. \tag{10}$$

Here, the subscript on a given quantity indicates the number of iterations. A simple criterion for achieving this iterative process is that the absolute values of all the constraints are kept below a desired small quantity ϵ : $\max(|C_1|, |C_2|, \dots, |C_N|)_i < \epsilon$. If the CVs are suitably estimated at the beginning of the iterative process ($i=0$), then only a few iterations will be sufficient to minimize the RFE. A good estimation of the CVs to start the process can be obtained by the following formulas:

$$X_1 = \max(|\psi|), \tag{11a}$$

$$X_2 = \frac{\int_{-\infty}^{\infty} (t|\psi|^2) dt}{\int_{-\infty}^{\infty} |\psi|^2 dt}, \tag{11b}$$

$$X_3 = \sqrt{2} \sqrt{\frac{1}{N1} L1 - X_2^2}; \quad N1 = \int_{-\infty}^{\infty} |\psi|^2 dt;$$

$$L1 = \int_{-\infty}^{\infty} (t^2 |\psi|^2) dt, \tag{11c}$$

$$X_4 = i \frac{\int_{-\infty}^{\infty} (t \psi^* \psi_t) dt}{\int_{-\infty}^{\infty} (t^2 \psi^* \psi_t) dt} + \text{c.c.}, \tag{11d}$$

$$X_5 = \frac{\int_{-\infty}^{\infty} (w |\tilde{\psi}|^2) dw}{\int_{-\infty}^{\infty} |\tilde{\psi}|^2 dw}, \tag{11e}$$

$$X_6 = 0. \tag{11f}$$

In Eq. (11e), $\tilde{\psi}$ represents the spectral Fourier transform of ψ . Thus, it is quite clear that the amount of calculations required by the direct minimization of the RFE to obtain the values for the CVs, represent only a small fraction of the calculations which are required when solving directly the equations of motion (7) and (9). However, more importantly, the CV equations of motion allow one to proceed further in analytical investigations [43].

TABLE I. Fiber parameters.

	Dispersion (ps/nm km)	Slope (ps/nm ² km)	Loss (dB/km)	A_{eff} (μm^2)	n_2 (m ² /W)
SMF	17	0.057	0.20	80	2.7×10^{-20}
DCF	-80	-0.175	0.6	20	2.55×10^{-20}

IV. APPLICATION OF THE CV THEORY

A. Single-soliton dynamics

In Ref. [43], to illustrate the CV treatment for DM solitons, we have demonstrated the single-pulse propagation in a typical DM fiber transmission line, with a periodic dispersion management using two types of fiber, namely single-mode fiber (SMF) and dispersion-compensating fiber (DCF). The dispersion map is made up of 8.75-km length of SMF fiber and 1.835-km length of DCF fiber. We have performed the calculations on the basis of the parameters for SMF and DCF fibers as mentioned in Table I. Parameter T_R for both types of fibers is taken as 1.422 fs. We have also carried out the numerical simulations not presented here, and found that our complete CV theory, bare approximation (or variational equations), and direct RFE minimization (described in Sec. III) essentially give the same result even for the pulse propagation over transoceanic distances (6000 km) with negligible values for the RFE.

Thus, we believe that a careful analysis of the lowest-order approximation equations (A7) should provide maximum insight for the dynamics due to any detrimental effects such as optical losses, third-order dispersion, stimulated Raman scattering, and self-steepening in DM transmission lines. Whereas the bare approximation based on the Gaussian ansatz agrees very well with the full CV theory for the single-pulse dynamics in the above DM transmission line, this approximation may in contrast lead to very poor result in some other problems, such as the modeling of soliton interactions, as we discuss below.

B. Intrachannel pulse interactions

In this subsection, we discuss the problem of introducing the CVs in the NLSE in view of modeling the interaction of adjacent pulses in the same channel of a transmission system. Fundamentally, optical solitons in fibers do not possess a compact support. In other words, DM solitons are characterized (theoretically) by infinite wings that cause mutual interactions between adjacent solitons in the same communication channel. This interaction, which can lead to the coalescence of adjacent soliton bits after a certain propagation distance, constitutes a main source of limitation in the maximum transmission distance in a single communication channel.

To study the interaction of two adjacent pulses, we decompose the original field in the same way as in Eq. (2) but with the following ansatz:

$$f = f_+ + f_-, \quad (12)$$

where

$$f_{\pm}(t, z) = X_1 \exp \left[-\frac{(t \pm X_2)^2}{X_3^2} + i \frac{X_4}{2} (t \pm X_2)^2 \mp i X_5 (t \pm X_2) + i X_6 \right]. \quad (13)$$

An analytical procedure that is commonly used to obtain the CV equations of motion corresponds to a quasiparticle approach in which one considers each individual pulse as being weakly perturbed by the other pulse [2,23,26,35,49]. Mathematically, the original field ψ is taken as a linear superposition of two one-soliton fields:

$$\psi = u_1 + u_2. \quad (14)$$

Next, the nonlinear term $|\psi|^2 \psi$ is split into two parts as follows:

$$|\psi|^2 \psi = (|u_1|^2 u_1 + 2|u_1|^2 u_2 + u_1^2 u_2^*) + (|u_2|^2 u_2 + 2|u_2|^2 u_1 + u_2^2 u_1^*). \quad (15)$$

If one considers that only the tails are interacting, then one can split the NLSE into two equations for the evolution of u_l :

$$\frac{\partial u_l}{\partial z} + i \frac{\beta_2}{2} \frac{\partial^2 u_l}{\partial t^2} - i \gamma |u_l|^2 u_l + \frac{\alpha}{2} u_l = i \gamma (2|u_l|^2 u_{3-l} + u_l^2 u_{3-l}^*), \quad (16)$$

where l ($= 1, 2$) denotes each pulse. An important point to be noticed here is that the cross-phase modulation (XPM) term $2|u_{3-l}|^2 u_l$ has been neglected in Eq. (16), which is hereafter referred to as the “*reduced intrachannel NLSE*.” Then, applying the bare approximation to the reduced intrachannel NLSE, that is, substituting $u_l = f_{\pm}$ in Eq. (16), and projecting the resulting equation in the direction of $\partial u_l^* / \partial X_k$ yields

$$\dot{X}_1 = \frac{1}{2} (\beta_2 X_1 X_4 - \alpha X_1) - \frac{\gamma X_1^2 E}{8\sqrt{2}} [(10 - 4X_2^2/X_3^2 + X_3^2 X_2^2 X_4^2 - 2X_3^2 X_2 X_4 X_5 + X_3^2 X_5^2) s + 4X_2 (X_2 X_4 - X_5) c], \quad (17a)$$

$$\dot{X}_2 = -\beta_2 X_5 + \frac{\gamma X_1^2 E}{2\sqrt{2}} [X_3^2 (X_2 X_4 - X_5) c + 2X_2 s], \quad (17b)$$

$$\dot{X}_3 = -\beta_2 X_3 X_4 + \frac{\gamma X_1^2 E}{4\sqrt{2}} [4X_2 X_3 (X_2 X_4 - X_5) c + (X_3^3 X_2^2 X_4^2 - 2X_3^3 X_2 X_4 X_5 - 4X_2^2/X_3 + 2X_3 + X_3^3 X_5^2) s], \quad (17c)$$

$$\begin{aligned} \dot{X}_4 = & -\beta_2 \left(\frac{4}{X_3^4} - X_4^2 \right) - \frac{\sqrt{2} \gamma X_1^2}{X_3^2} + \frac{\gamma X_1^2 E}{3\sqrt{2}} \left[9 \left(2X_2 X_4 X_5 \right. \right. \\ & \left. \left. - X_2^2 X_4^2 + \frac{4X_2^2}{X_3^4} - \frac{2}{X_3^2} - X_5^2 \right) c + \frac{X_2}{X_3^2} (X_2 X_4 - X_5) s \right], \end{aligned} \quad (17d)$$

$$\begin{aligned} \dot{X}_5 = & \frac{\gamma X_1^2 E}{2\sqrt{2}} \left[\left(X_4 X_3^2 X_5 - \frac{12X_2}{X_3^2} - X_4^2 X_3^2 X_2 \right) c \right. \\ & \left. + 2(3X_5 - 2X_2 X_4) s \right], \end{aligned} \quad (17e)$$

$$\begin{aligned} \dot{X}_6 = & -\beta_2 \left(\frac{X_5^2}{2} - \frac{1}{X_3^2} \right) + \frac{5\gamma X_1^2}{4\sqrt{2}} + \frac{\gamma X_1^2 E}{8\sqrt{2}} [4X_2(5X_5 - 3X_2 X_4) s \\ & + (30 - 10X_3^2 X_2 X_4 X_5 + 7X_3^2 X_5^2 - 12X_2^2/X_3^2 \\ & + 3X_3^2 X_2^2 X_4^2) c], \end{aligned} \quad (17f)$$

where

$$s = \sin[(X_2 X_4 - X_5) X_2],$$

$$c = \cos[(X_2 X_4 - X_5) X_2],$$

$$E = \exp[-1/4(X_3^4 X_2^2 X_4^2 - 2X_3^4 X_2 X_4 X_5 + X_3^4 X_5^2 + 12X_2^2)/X_3^2].$$

Thus, the CV equations of motion (17), which we henceforth refer to as the “*reduced intrachannel bare calculation*,” are equivalent to the averaged Lagrangian approach used in Ref. [35]. Knowing that two distinct approximation schemes (which neglect the XPM terms and the soliton dressing, respectively) are made in the reduced intrachannel BC (bare calculation), it is difficult to ascertain precisely the particular effect of any of these two types of approximations by simply comparing the results from the reduced intrachannel BC to the full CV theory (including the soliton dressing in the NLSE). In this context, it is useful to carry out a *full* bare calculation using the NLSE (1) [instead of the reduced intrachannel NLSE (16)]. Substituting the ansatz $f = f_+ + f_-$ in the NLSE (1) with losses and gain, and projecting the resulting equation in the direction of $\partial f^*/\partial X_k$ yields the CV equations in the following matrix form:

$$[\dot{X}] = [M]^{-1} [F], \quad (18)$$

where the matrices $[M]$ and $[F]$ are given explicitly in Appendix B. Note that the reduced intrachannel BC (17) has the convenient feature of requiring much fewer algebraic manipulations than the full bare calculation (18). Figure 1 represents the dynamics of two pulses, with the arbitrary initial conditions $[X_1 = 0.23, X_2 = \pm \Delta_0/2, X_3 = 9.88, X_4 = -0.0079, X_5 = 0, X_6 = 0]$. The initial pulse separation $\Delta_0 = 2X_2 = 16$ ps and 28.5 ps represent approximately 1.4 times and 2.4 times the initial pulse width ($T_0 = 11.6$ ps FWHM). In all the pictures of the present section, the solid

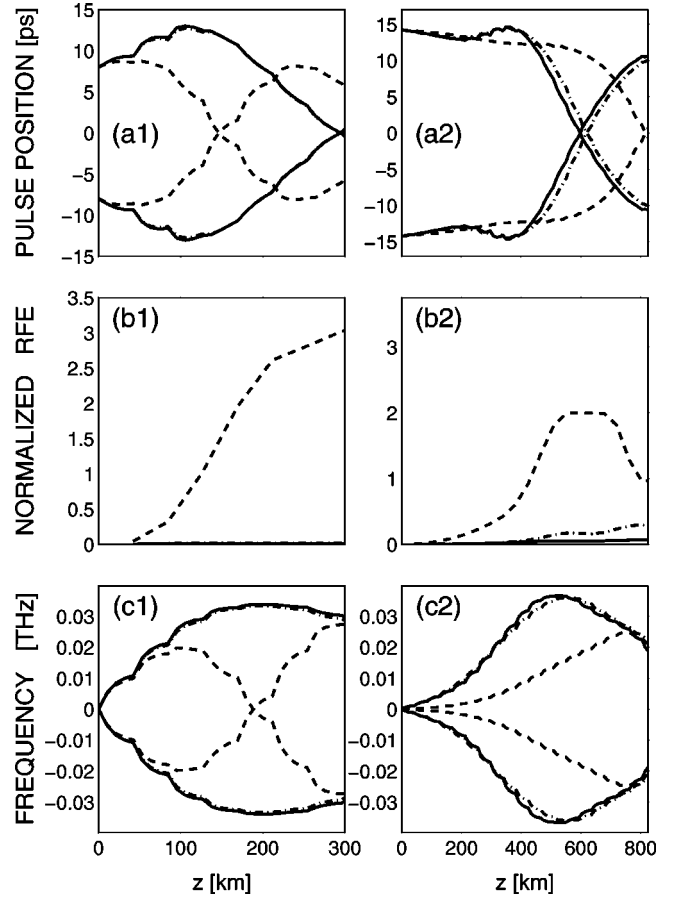


FIG. 1. Plots showing an intrachannel pulse interaction. (a) Evolution of the pulse positions versus propagation coordinate z . (b) Evolution of the normalized residual-field energy $\Lambda(z)/E(0)$ versus propagation coordinate z . (c) Evolution of the frequency versus propagation coordinate z . Solid, dot-dashed, and dashed curves correspond to full CV theory, the full bare calculation, and the reduced intrachannel bare calculation, respectively.

curves represent the results obtained from the numerical procedure of minimization of the RFE described in Sec. III, which will be hereafter referred to as the “*full CV theory*.” The dot-dashed and dashed curves will represent the full and reduced intrachannel BCs, respectively. Figure 1 demonstrates the general feature that the BCs based on the Gaussian ansatz lead to much less fair results for the modeling of soliton interactions than for the single-soliton dynamics (discussed in the earlier subsection). Figures 1 (a1), (b1), and (c1) [which correspond to $\Delta_0 = 16$ ps] and 1 (a2), (b2), and (c2) ($\Delta_0 = 28.5$ ps), respectively, represent situations where the two input pulses strongly and weakly overlap with each other. For example, we observe in Fig. 1 (a1) the following prediction for the collision distance: $Z_c = 294.7$ km (given by the full CV theory). The full BC leads to $Z_c = 294.6$ km, which therefore agrees extremely well with the full CV theory. The reduced intrachannel BC ($Z_c = 146.5$ km) leads to a huge discrepancy, of nearly 50%. Then the question arises: where does this huge discrepancy come from? To answer this question, we have applied our CV treatment (based on the residual field minimization) to the reduced

NLSE (16) and found essentially the same results as for the CV treatment of the NLSE (1), as represented by the solid curves in Fig. 1. We thus deduce that the large discrepancy mentioned above results mostly from the approximate nature of the corresponding BC with Gaussian ansatz in Eq. (17). Indeed the stability of a given BC (i.e., its ability to accurately follow the exact pulse trajectory in parameter space) is determined not only by the type of ansatz considered but also by the particular type of nonlinear partial differential equation that describes the dynamics. The results in Fig. 1 reveal that the BC for the reduced NLSE (16) with a Gaussian ansatz is highly unstable compared with the BC for the NLSE (1). Figures 1 (b1) and (b2) show the spatial evolution of the normalized RFE for the three CV approaches. Note that the residual field is given by $q(z,t) = \psi(z,t) - f([X])$, where $\psi(z,t)$ is the exact DM soliton field obtained by numerically solving the NLSE (1). In all three cases, the RFE execute an oscillating behavior with an amplitude that increases continually as it approaches the collision point (for clarity, we have plotted only the envelope of the oscillating RFE). We reemphasize that the appearance of a residual field simply indicates that the Gaussian ansatz functions that we use do not correspond to the exact solution of the NLSE (1). More importantly, as one could have expected in view of the results in Figs. 1 (a1) and (a2), the reduced intrachannel BC leads to dramatically large values of the RFE [see the dashed curve in Figs. 1 (b1) and (b2)]. One can clearly observe in Fig. 1 (b1) a peak value that attains nearly 300% of the total energy of the two pulses, in the range $0 \leq z \leq Z_c$. The occurrence of these huge values of the RFE gives no physical meaning to the collective variables obtained via this reduced intrachannel BC. Quite in contrast, the full BC leads to a collision distance much more accurate than for the reduced intrachannel BC. We observe in Figs. 1 (a1), (b1), and (c1), where the solid and dot-dashed curves essentially coincide, that the full BC leads to excellent results in the case when the two input pulses strongly overlap. On the other hand, Figs. 1 (a2), (b2), and (c2) reveal that the agreement between the full BC and the full CV theory is not so good in the case where the input pulse weakly overlap (compared with the case of strong initial overlapping). Nevertheless, here, the level of the RFE for the full BC, which does not exceed 17% of the total energy of the two pulses [see Fig. 1 (b2)], corresponds to a good qualitative agreement. The full CV theory leads to a RFE that does not exceed 5% of the total energy of the two pulses over the whole collision distance [see the solid curves in Figs. 1 (b1) and (b2)], which therefore gives much better physical meaning to the corresponding CVs.

The above-mentioned features appear also clearly in Figs. 2(a) and 2(b), which represent the peak RFE over $0 \leq z \leq Z_c$, and the collision distance, respectively, as a function of the normalized initial pulse separation Δ_0/T_0 . Figure 2(a) shows that the reduced intrachannel BC leads to huge values of the RFE [dashed curve in Fig. 2(a)] compared to the full BC, in a wide region of initial pulse separation ranging from the case of weak to strong input-pulse overlap. On the other hand, we observe in Fig. 2(b) that for $\Delta_0/T_0 \approx 1.85$, the two BCs predict fortuitously well the collision distance. Nevertheless, one cannot conclude that the BCs are then effective.

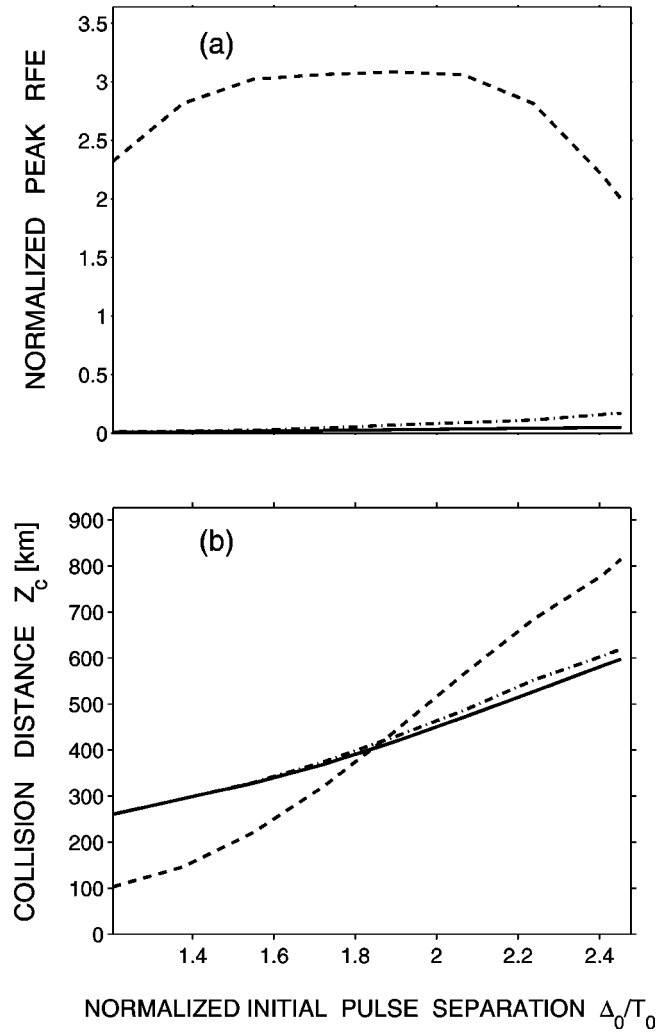


FIG. 2. (a) Evolution of the normalized residual-field energy $\Lambda(z)/E(0)$ versus normalized initial pulse separation Δ_0/T_0 . (b) Evolution of the collision distance Z_c versus normalized initial pulse separation Δ_0/T_0 . Solid, dot-dashed, and dashed curves correspond to full CV theory, the full bare calculation, and the reduced intrachannel bare calculation, respectively.

In particular, the reduced intrachannel BC leads to clearly wrong results in predicting the other soliton parameters (e.g., pulse width), as can be seen in Fig. 3; hence a high RFE [see Fig. 3(a)].

Thus, it comes out from the results of this subsection that the reduced intrachannel BC with the Gaussian ansatz describes very poorly the intrachannel pulse interactions. The full BC gives generally much better results, with an acceptable level of residual field. However, this full BC leads to a small discrepancy (with respect to the full CV theory) for large initial pulse separation. In such a situation, one must “dress” the Gaussian ansatz to obtain a fair quantitative prediction of the effects of intrachannel pulse interactions, or make use of an accurate ansatz (e.g., Hermite-Gaussian ansatz [44–46]).

C. Interchannel pulse interactions

In this subsection, we discuss the application of the CV theory to the problem of interchannel pulse interactions. A

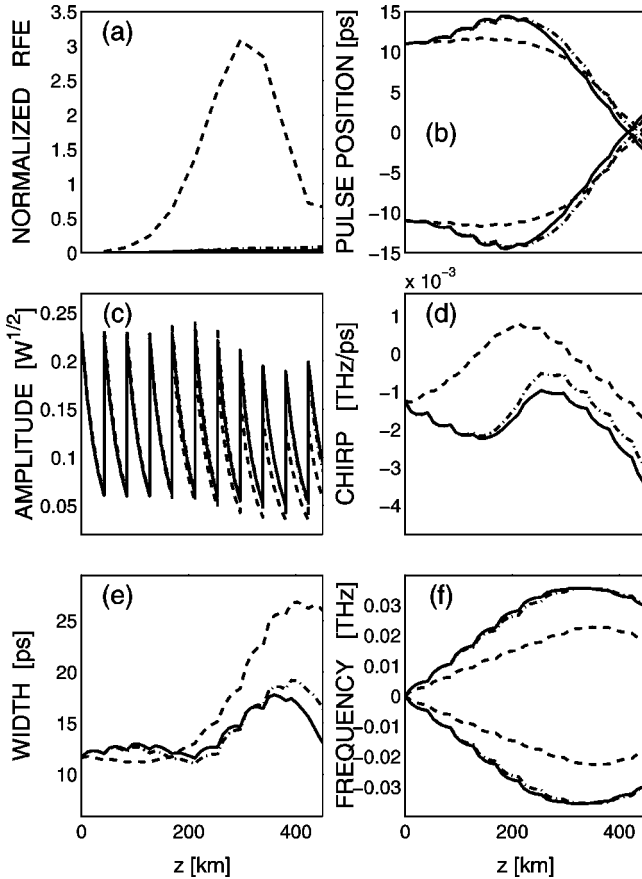


FIG. 3. Plots showing an intrachannel pulse interaction. (a) Evolution of the normalized residual-field energy $\Lambda(z)/E(0)$ versus propagation coordinate z . (b) Evolution of the pulse positions versus propagation coordinate z . (c),(d),(e),(f) Evolution of the pulse amplitude, chirp, width, and frequency versus propagation coordinate z . Solid, dot-dashed, and dashed curves correspond to full CV theory, the full bare calculation, and the reduced intrachannel bare calculation, respectively.

main source of limitation of the performance of WDM (wavelength-division multiplexing) systems lies in the effects induced by collisions between pulses propagating in different communication channels. Indeed, in soliton-based WDM systems, pulses that are launched in different channels propagate at different speeds, which leads inevitably to collisions between fast and slow pulses in long-distance transmissions. In particular, when two solitons collide in a lumped amplifier, their frequencies undergo a shift due to an amplification-induced imbalance between the local dispersion and nonlinearity. A permanent frequency shift induced by repeated collisions in DM systems may lead to significant timing jitter at the system output. Numerous recent studies demonstrate that such effects may be reduced by suitably optimizing the dispersion map [33,34,36,50–53]. It is not the subject of the present study to carry out such optimization processes, but rather to analyze the ability of CV treatments to accurately predict the effects of pulse interactions in WDM systems.

Here, the dynamics of each pulse is strongly influenced by the other pulse intensity. So the XPM term plays a major

role. Following the same principle as in the case of the intrachannel, one generally splits the NLSE into two equations for the evolution of u_l [2,26,33,34,36,54–56]:

$$\frac{\partial u_l}{\partial z} + i \frac{\beta_2}{2} \frac{\partial^2 u_l}{\partial t^2} - i \gamma |u_l|^2 u_l + \frac{\alpha}{2} u_l = 2i \gamma |u_{3-l}|^2 u_l. \quad (19)$$

An important point to be noticed here is that the four-wave mixing term $u_l^2 u_{3-l}^*$ has been neglected in Eq. (19), which is hereafter referred to as the “*reduced interchannel NLSE*.” Then, applying the bare approximation to the reduced interchannel NLSE, that is, substituting $u_l = f_{\pm}$ in Eq. (19), and projecting the resulting equation in the direction of $\partial u_l^* / \partial X_k$ yields

$$\dot{X}_1 = \frac{1}{2} (\beta_2 X_1 X_4 - \alpha X_1), \quad (20a)$$

$$\dot{X}_2 = -\beta_2 X_5, \quad (20b)$$

$$\dot{X}_3 = -\beta_2 X_3 X_4, \quad (20c)$$

$$\begin{aligned} \dot{X}_4 = & -\beta_2 \left(\frac{4}{X_3^4} - X_4^2 \right) - \frac{\sqrt{2} \gamma X_1^2}{X_3^2} - \gamma \frac{\sqrt{2}}{2 X_3^4} (4 X_1^2 X_3^2 \\ & - 32 X_1^2 X_2^2) \exp(-4 X_2^2 / X_3^2), \end{aligned} \quad (20d)$$

$$\dot{X}_5 = -4 \sqrt{2} \gamma \frac{X_1^2 X_2}{X_3^2} \exp(-4 X_2^2 / X_3^2), \quad (20e)$$

$$\begin{aligned} \dot{X}_6 = & -\beta_2 \left(\frac{X_5^2}{2} - \frac{1}{X_3^2} \right) + \frac{5 \gamma X_1^2}{4 \sqrt{2}} + \frac{\gamma}{8 X_3^2} (\sqrt{102} X_3^2 X_1^2 \\ & - \sqrt{162} X_1^2 X_2^2) \exp(-4 X_2^2 / X_3^2). \end{aligned} \quad (20f)$$

Thus, the CV equations of motion (20), which we henceforth refer to as the “*reduced interchannel bare calculation*,” are equivalent to the averaged Lagrangian approach used in Refs. [34,36,54].

To illustrate our demonstration, we consider the case where two given pulses are launched with a temporal separation of $\Delta_0 = 250$ ps in two channels spaced by $\Delta \nu = 150$ GHz, in a DM line of total length $L = 2000$ km. Figure 4 shows the evolution of the pulse parameters during this collision process. The solid, dashed, and dot-dashed curves represent the full CV theory, reduced interchannel BC, and full BC, respectively. Figure 4(a) shows that the collision occurs at $Z_c \approx 1110$ km. Note that the pulses execute a zig-zag motion that causes repeated collisions in a region around Z_c (with full pulse overlapping) before they separate. An important parameter that serves as a measure of the importance of the effects of the collision is the *timing shift*: $\delta X_2(Z) \equiv X_2 - (-\pi \Delta \nu \langle \beta_2 \rangle |z + \Delta_0/2|)$, represented in Fig. 4(b). The parameter $\langle \beta_2 \rangle = -2.35 \times 10^{-4}$ ps²/m represents the average dispersion of the line. One can clearly observe in Fig. 4(b) that the two pulses interact in fact over a relatively large distance ranging from $z \approx 600$ km to $z \approx 1700$ km,

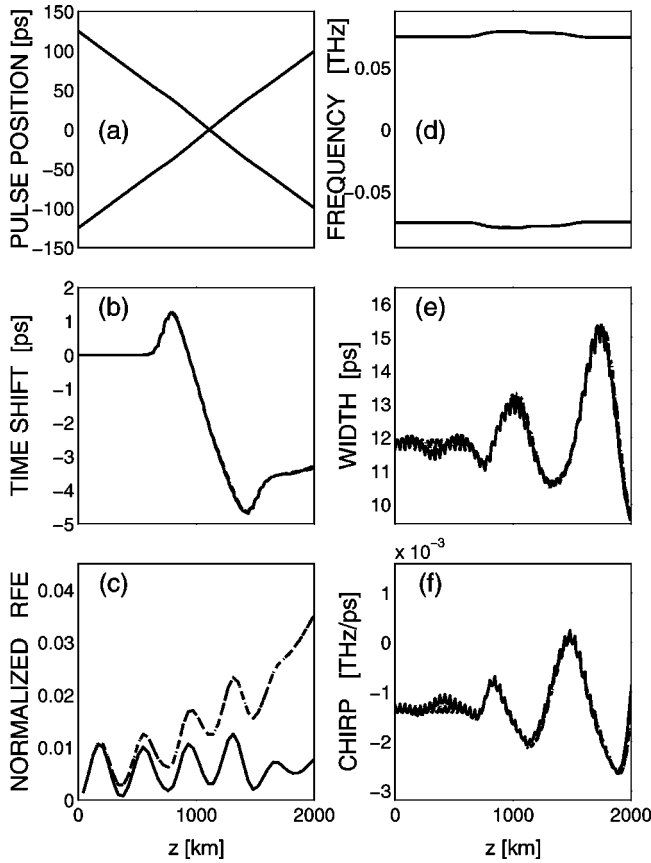


FIG. 4. Plots showing an interchannel pulse interaction for $\Delta_0 = 250$ ps and $\Delta\nu = 150$ GHz. (a) Evolution of the pulse positions versus propagation coordinate z . (b) Time shift δX_2 versus propagation coordinate z . (c) Normalized residual-field energy versus propagation coordinate z . (d),(e),(f) Evolution of the frequency, width, and chirp versus z . Solid, dot-dashed, and dashed curves correspond to full CV theory, the full bare calculation, and the reduced interchannel bare calculation, respectively.

through the cross-phase modulation. Using the full CV theory, we find that the interaction leads to a timing shift of $\delta X_2(L) = -3.3$ ps, and a permanent frequency shift $\delta \tilde{X}_5 = [X_5(L) - X_5(0)]/2\pi = 0.46$ GHz. At the same time, the interaction causes pulse parameters—width and chirp—to execute relatively large-amplitude oscillations around their initial values, as can be seen in Figs. 4(e) and 4(f). The correctness of the above CV treatments is measured through the level of the RFE represented in Fig. 4(c). We observe the following general features. First, the full CV theory (solid curve) leads to the smallest RFE, with a peak value that represents only 1% of the total energy of the two pulses. This indicates that our procedure of minimizing the soliton “dressing” provides an excellent description of the interchannel pulse interactions. Second, the reduced inter-channel and full BCs yield essentially the same result, as Fig. 4 shows, thus implying that the reduced interchannel NLSE (19) and the reduced interchannel BC (20) provide an approximate but highly accurate description of pulse propagation in well spaced channels. In fact, the ability of the reduced interchannel BC with Gaussian ansatz, to accurately describe pulse propagation in systems with well-spaced

channels, was already reported in previous studies [28,32–36]. Thus, our study of the RFE for the reduced interchannel BC [dashed curve in Fig. 4(c)] confirms the previous studies. In such cases where the BC gives excellent results, there is no need to *dress* the Gaussian ansatz, and the use of the reduced interchannel NLSE or the reduced interchannel BC (or any similar variational approach) is fully justified [28,32–36].

A way to increase the capacity of soliton-based communication systems lies in the use of very closely spaced signal wavelengths. This technique is commonly exploited for setting up the so-called “dense” WDM systems [57,58]. It is interesting to examine the case of extremely close channels, but where the individual identities of the channels are preserved throughout the pulse transmission. To this end, we have carried out a simulation of the interaction of two pulses in the same conditions as in Fig. 4 but with a smaller frequency spacing between the two channels: $\Delta\nu = 100$ GHz. The results are displayed in Fig. 5, where the solid, dot-dashed, and dashed curves represent the full CV theory, the full BC, and the reduced interchannel BC, respectively. Figure 5 exhibits two distinct regimes of the system behavior.

(i) First, we observe in Figs. 5(a) and 5(b) a regime of low-amplitude for the residual field, which takes place from $z=0$ up to the collision point $z=Z_c \approx 1646$ km. Indeed, in this regime, the RFE predicted by the full CV theory does not exceed 1.5% of the total energy of the system, thus indicating that the Gaussian ansatz function provides a fairly good representation of the exact solution of the NLSE (1). In fact, the shape of the two pulses remains quite close to a Gaussian profile from $z=0$ up to a few hundred km after the collision. This leads to fairly accurate bare calculations, with a normalized RFE that does not exceed 3%.

(ii) Now, from $z=Z_c$ upwards we observe in Figs. 5(a) and 5(b) a regime of high-amplitude for the residual field, characterized by large values of the RFE. This behavior indicates that this collision process causes a severe distortion of the pulse (with respect to the initial Gaussian profile). The resulting increase of the RFE differs qualitatively depending on the CV treatment considered. In particular, we observe in Fig. 5(b) that the bare calculations lead to a RFE that increases continually for $z \geq Z_c$, with peak values that grow up to 120% of the total energy of the system. Such huge values of the RFE give no physical meaning to the corresponding CVs at the system’s output. In other words, the BCs lead there to wrong results at the system’s output. On the other hand, as the solid curve in Fig. 5(b) shows, the full CV theory leads to a RFE that increases continually from $z = Z_c$ up to $z \approx 2500$ km before stabilizing around $\approx 13\%$ during the remaining propagation distance. This level of the RFE is one order of magnitude lower than that obtained from the bare calculations. Thus, the stabilization of the RFE within 13%, is a benefit effect of the process of minimization of the residual field in the full CV theory. Nevertheless, the value of 13% for the RFE is still relatively large to guarantee a fair quantitative prediction of the actual pulse behavior at the system’s output. The agreement here is mainly qualitative. In particular, Figs. 5(e) and 5(f), which we obtained by solving the NLSE (1), show the exact profiles of the two

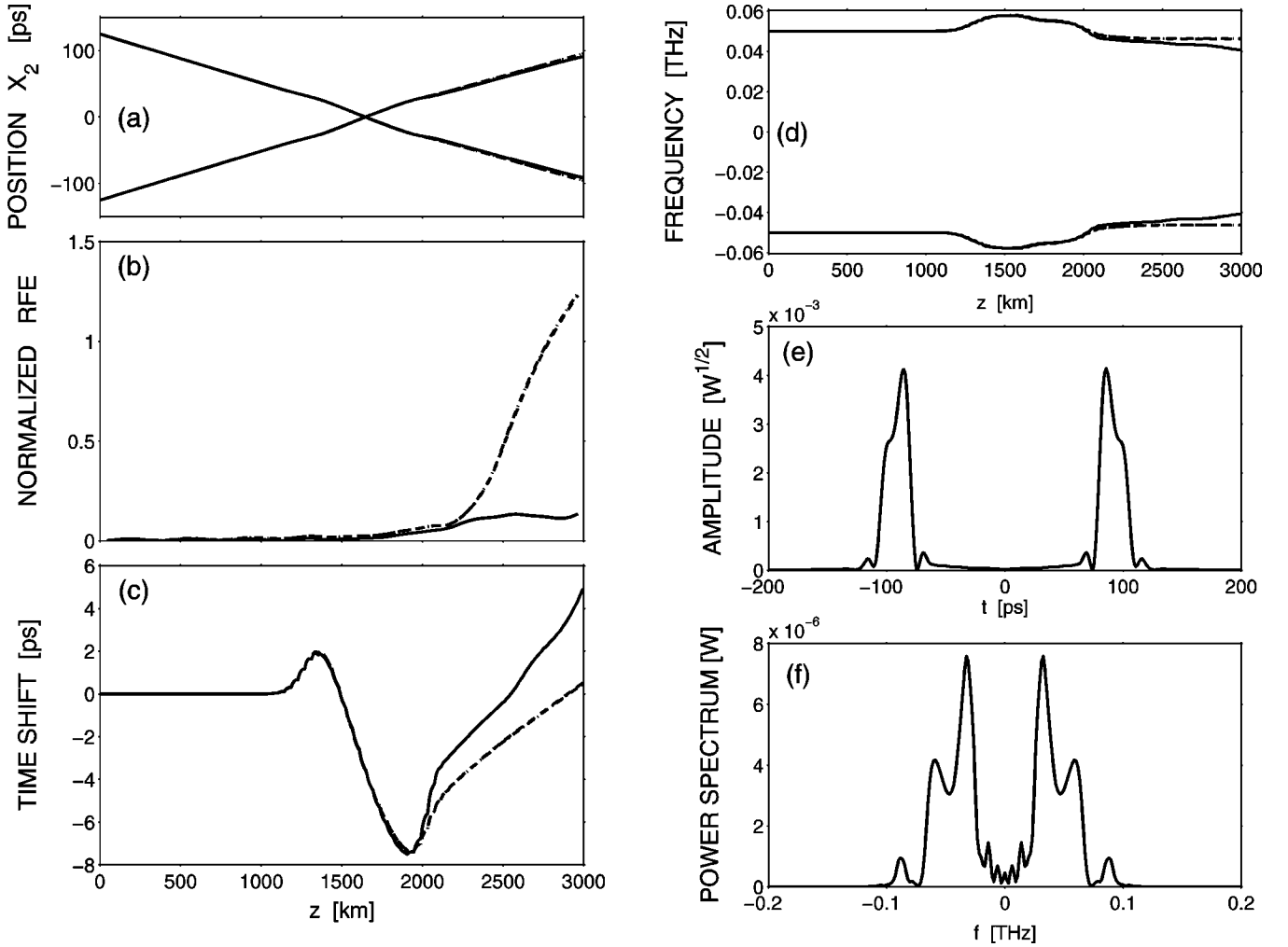


FIG. 5. Plots showing an interchannel pulse interaction for $\Delta_0=250$ ps and $\Delta\nu=100$ GHz.

output pulses and the corresponding frequency spectrum, respectively. One can clearly observe, as predicted by the full CV theory, that the pulses are severely distorted with respect to a Gaussian profile; hence a large RFE.

As a general remark on all the above examples of applications of the CV theory to DM systems, it comes out that the BC (or similar variational approaches) describes more or less well the pulse propagation depending on the particular situation under consideration. On one hand, the BC with Gaussian ansatz provides a fair quantitative description of the system's behavior in case of a single-pulse propagation in a DM line [43], and in the case of two pulses interacting in well spaced communication channels. In such cases, there is no need to dress the Gaussian ansatz. Another useful advantage of the BC is that it requires only a small fraction of the amount of calculations required when using a full CV approach. On the other hand, we have observed that the BC with Gaussian ansatz provides either very poor results or completely wrong results, in predicting the system's behavior in case of intrachannel pulse interactions and when two pulses interact in very closely spaced channels. In such cases, one must either make use of more accurate ansatz functions, or dress the Gaussian ansatz to fairly describe the behavior of optical solitons in fibers.

V. CONCLUSION

In the present work, we have developed a rigorous CV treatment for the generalized NLSE for the propagation of optical soliton in fibers, using a projection-operator formalism. We have described the essential steps for obtaining the CV equations of motion. The first fundamental point of the present work, which makes the greatest qualitative difference with respect to all other previous CV treatments of the NLSE, lies in the fact that we have introduced a residual field q accounting for the dressing of the soliton and any radiation coupled to the soliton's motion. The second fundamental point of our CV approach lies in the introduction of constraints, $C_j \approx 0$, Eq. (5), on the CVs X_j ($j=1, \dots, N$), which give proper physical meaning for the CVs by configuring the ansatz function $f(X_1, X_2, \dots, X_N)$ to be a best fit to the original field variable ψ . The main virtue of this CV approach is to make the derivation of the CV equations of motion relatively simple. Finally we have also demonstrated the application of this CV theory for a typical DM fiber link. Although we have focussed on the two-soliton dynamics, the CV theory presented in this paper can be straightforwardly extended to a general multisoliton dynamics. In particular, the generalized NLSE can be used to describe the dynamics

of soliton packet in WDM or time division multiplexing transmission systems. For example, the dynamics of a given number of solitons, say M , propagating in different channels of a WDM system may be effectively handled in the CV theory by expressing the ansatz function f as a linear superposition of one-soliton ansatz,

$$f = \sum_{n=1}^M f_n(X_{1n}, X_{2n}, X_{3n}, X_{4n}, X_{5n}, X_{6n}), \quad (21)$$

where X_{1n} , X_{2n} , X_{3n} , X_{4n} , X_{5n} , and X_{6n} represent the soliton amplitude, temporal position, width, chirp, frequency, and phase, respectively, in the n th channel with frequency $\omega_n = X_{5n}/(2\pi)$. With the above ansatz, the generalized NLSE can be expressed in terms of CVs X_{jn} , exactly as we have done for the two-soliton case. From a practical point of view, the information that may be gained now from this CV treatment of the generalized NLSE should provide a deep insight into detrimental effects that cause instability processes on optical solitons in fibers. This CV approach can therefore be exploited for the optimization of fiber transmission lines in optical communications.

ACKNOWLEDGMENTS

The Centre National de la Recherche Scientifique and the Ministère de l'Éducation Nationale de la Recherche et de la Technologie (Contract ACI Jeunes No. 2015) are gratefully acknowledged for their financial support of this work. The work of K. Nakkeeran has been supported by the research project sponsored by Conseil Régional de Bourgogne. The authors would also like to thank S. Wabnitz and G. Millot for fruitful discussions.

APPENDIX A: AVERAGED LAGRANGIAN APPROACH

In this appendix, we briefly present the essential steps that are needed to express the generalized NLSE in terms of CVs, using the perturbed Lagrangian approach. We consider the generalized NLSE in the form

$$\psi_z + i \frac{\beta_2(z)}{2} \psi_{tt} - i \gamma(z) |\psi|^2 \psi = \epsilon R, \quad (A1)$$

where

$$\begin{aligned} \epsilon R = & -\frac{\alpha(z)}{2} \psi + \frac{\beta_3(z)}{6} \psi_{ttt} - i \gamma_r(z) \psi (|\psi|^2)_t \\ & - \gamma_s(z) (|\psi|^2 \psi)_t. \end{aligned} \quad (A2)$$

The Lagrangian for Eq. (A1) without perturbation term ($\epsilon R = 0$) is given by

$$L = \int_{-\infty}^{\infty} \left[\frac{\beta_2(z)}{2} |\psi_t|^2 + \frac{\gamma(z)}{2} |\psi|^4 + \frac{i}{2} (\psi^* \psi_z - \psi \psi_z^*) \right] dt. \quad (A3)$$

Substituting the Gaussian ansatz function f given by

$$f = X_1 \exp \left[-\frac{(t-X_2)^2}{X_3^2} + i \frac{X_4}{2} (t-X_2)^2 + i X_5 (t-X_2) + i X_6 \right], \quad (A4)$$

where X_1 , X_2 , $\sqrt{2 \ln 2} X_3$, $X_4/(2\pi)$, $X_5/(2\pi)$, and X_6 represent the pulse amplitude, temporal position, pulse width (FWHM), chirp, frequency, and phase, respectively, in Eq. (A3), and performing the integration leads to the following Lagrange function of the CVs:

$$\begin{aligned} L = & \frac{\sqrt{\pi}}{2\sqrt{2}} \beta_2(z) X_1^2 \left(\frac{1}{X_3} + \frac{X_3^3 X_4^2}{4} + X_3 X_5^2 \right) + \frac{\sqrt{\pi}}{4} \gamma(z) X_3 X_1^4 \\ & - \frac{\sqrt{\pi}}{8\sqrt{2}} X_1^2 X_3^3 \dot{X}_4 - \frac{\sqrt{\pi} X_1^2 X_3}{\sqrt{2}} (\dot{X}_6 + X_5 \dot{X}_2) \\ & - X_1^2 X_3^2 [\beta_2(z) X_4 X_5 - X_4 \dot{X}_2 - \dot{X}_5]. \end{aligned} \quad (A5)$$

Then, the variational equations are written as

$$\frac{\partial L}{\partial X_j} - \frac{d}{dz} \left(\frac{\partial L}{\partial \dot{X}_j} \right) = \int_{-\infty}^{\infty} \epsilon R \frac{\partial f^*}{\partial X_j} + \text{c.c.} \quad (A6)$$

Substituting the ansatz function f in ϵR [i.e., setting $\psi = f$ in Eq. (A2)], and performing the integration of the right-hand side of Eq. (A6), we obtain the following variational equations:

$$\dot{X}_1 = -\frac{1}{2} \alpha(z) X_1 + \frac{1}{2} \beta_2(z) X_1 X_4 - \frac{1}{2} \beta_3(z) X_1 X_4 X_5, \quad (A7a)$$

$$\begin{aligned} \dot{X}_2 = & -\beta_2(z) X_5 + \beta_3(z) \left(\frac{1}{2X_3^2} + \frac{X_5^2}{2} + \frac{X_3^2 X_4^2}{8} \right) \\ & + \frac{3}{2\sqrt{2}} \gamma_s(z) X_1^2, \end{aligned} \quad (A7b)$$

$$\dot{X}_3 = -\beta_2(z) X_3 X_4 + \beta_3(z) X_3 X_4 X_5, \quad (A7c)$$

$$\begin{aligned} \dot{X}_4 = & -\beta_2(z) \left(\frac{4}{X_3^4} - X_4^2 \right) - \frac{\sqrt{2} \gamma(z) X_1^2}{X_3^2} \\ & + \beta_3(z) \left(\frac{4X_5}{X_3^4} - X_4^2 X_5 \right) + \frac{\sqrt{2} \gamma_s(z) X_1^2 X_5}{X_3^2}, \end{aligned} \quad (A7d)$$

$$\dot{X}_5 = \frac{\sqrt{2} \gamma_r(z) X_1^2}{X_3^2} + \frac{\gamma_s(z) X_1^2 X_4}{\sqrt{2}}, \quad (A7e)$$

$$\begin{aligned} \dot{X}_6 = & \beta_2(z) \left(\frac{1}{X_3^2} - \frac{X_5^2}{2} \right) + \frac{5\gamma(z)X_1^2}{4\sqrt{2}} \\ & + \beta_3(z) \left(\frac{X_5^3}{3} + \frac{X_3^2 X_4^2 X_5}{8} - \frac{X_5}{2X_3^2} \right) + \frac{\gamma_s(z)X_1^2 X_5}{4\sqrt{2}}. \end{aligned} \quad (\text{A7f})$$

The above equations (A7) are exactly same as Eqs. (14) of Ref. [43]. Thus, the perturbed Lagrangian approach corresponds to the lowest-order approximation of the projection-operator approach. More importantly, in nonlinear fiber optics, there exist a host of nonlinear partial differential equations, which do not possess the Lagrangian function. In such cases, one cannot apply the Lagrangian approach, whereas the projection-operator approach can be used in all cases for obtaining the CV equations of motion without the help of the Lagrangian function.

APPENDIX B: FULL BARE CALCULATION

In this appendix, we present the full bare calculations. Substituting the ansatz

$$f = f_+ + f_-, \quad (\text{B1})$$

where

$$\begin{aligned} f_{\pm}(t, z) = & X_1 \exp \left[-\frac{(t \pm X_2)^2}{X_3^2} + i \frac{X_4}{2} (t \pm X_2)^2 \right. \\ & \left. \mp i X_5 (t \pm X_2) + i X_6 \right] \end{aligned} \quad (\text{B2})$$

in the NLSE (1) with losses and gain, and projecting the resulting equation in the direction of $\partial f^* / \partial X_k$ yields the CV equations in the following matrix form:

$$[\dot{X}] = [M]^{-1} [F], \quad (\text{B3})$$

where the matrices $[M]$ and $[F]$ are explicitly given by

$$[M] = \begin{pmatrix} m_{11} & m_{12} & m_{13} & m_{14} & m_{15} & 0 \\ m_{12} & m_{22} & m_{23} & m_{24} & m_{25} & m_{26} \\ m_{13} & m_{23} & m_{33} & 0 & m_{35} & m_{36} \\ m_{14} & m_{24} & 0 & m_{44} & m_{45} & m_{46} \\ m_{15} & m_{25} & m_{35} & m_{45} & m_{55} & m_{56} \\ 0 & m_{26} & m_{36} & m_{46} & m_{56} & m_{66} \end{pmatrix},$$

$$[F] = \begin{pmatrix} \frac{\beta_2(z)}{2} F_{11} + \gamma(z) F_{21} - \frac{\alpha(z)}{2} F_{31} \\ \frac{\beta_2(z)}{2} F_{12} + \gamma(z) F_{22} - \frac{\alpha(z)}{2} F_{32} \\ \frac{\beta_2(z)}{2} F_{13} + \gamma(z) F_{23} - \frac{\alpha(z)}{2} F_{33} \\ \frac{\beta_2(z)}{2} F_{14} + \gamma(z) F_{24} - \frac{\alpha(z)}{2} F_{34} \\ \frac{\beta_2(z)}{2} F_{15} + \gamma(z) F_{25} - \frac{\alpha(z)}{2} F_{35} \\ \frac{\beta_2(z)}{2} F_{16} + \gamma(z) F_{26} - \frac{\alpha(z)}{2} F_{36} \end{pmatrix}, \quad (\text{B4})$$

where

$$m_{11} = \sqrt{2} X_3 (1 + E_1),$$

$$m_{12} = \frac{X_1}{\sqrt{2}} E_1 (-X_3^4 X_4^2 X_2 + X_3^4 X_4 X_5 - 4X_2) / X_3,$$

$$\begin{aligned} m_{13} = & \frac{X_1}{\sqrt{2}} [1 - E_1 (-X_3^2 - 2X_3^4 X_2 X_4 X_5 + X_3^4 X_5^2 - 4X_2^2 \\ & + X_3^4 X_2^2 X_4^2) / X_3^2], \end{aligned}$$

$$m_{14} = \frac{X_1}{\sqrt{2}} X_2 X_3^3 E_1 (-X_2 X_4 + X_5),$$

$$m_{15} = -\frac{X_1}{\sqrt{2}} X_3^3 E_1 (-X_2 X_4 + X_5),$$

$$\begin{aligned} m_{22} = & \frac{X_1^2}{2\sqrt{2}} [(4X_3^2 + X_3^6 X_4^2 + 4X_3^4 X_5^2) / X_3^3 + E_1 (X_3^8 X_4^2 X_5^2 - X_3^6 X_4^2 \\ & + X_3^8 X_4^4 X_2^2 - 2X_3^8 X_4^3 X_2 X_5 + 16X_2^2 - 4X_3^2 + 8X_3^4 X_2^2 X_4^2 \\ & - 8X_3^4 X_2 X_4 X_5) / X_3^3], \end{aligned}$$

$$\begin{aligned} m_{23} = & -\frac{X_1^2}{2\sqrt{2}} E_1 (16X_2^3 - 4X_2 X_3^2 + 4X_2^2 X_4 X_5 X_3^4 - 4X_2 X_5^2 X_3^4 \\ & + 3X_3^6 X_4^2 X_2 - 3X_3^6 X_4 X_5 - X_3^8 X_4^4 X_2^3 + 3X_3^8 X_4^3 X_2^2 X_5 \\ & - 3X_3^8 X_4^2 X_2 X_5^2 + X_3^8 X_4 X_5^3) / X_3^4, \end{aligned}$$

$$\begin{aligned} m_{24} = & \frac{X_1^2}{4\sqrt{2}} [-X_3^3 X_5 + X_3 (-8X_5 X_2^2 + 8X_4 X_2^3 + 2X_3^2 X_5 \\ & + 2X_3^4 X_5^2 X_2 X_4 - 4X_3^2 X_4 X_2 + 2X_3^4 X_4^3 X_2^3 \\ & - 4X_3^4 X_5 X_2^2 X_4^2) E_1], \end{aligned}$$

$$m_{25} = -\frac{X_1^2}{2\sqrt{2}}[X_3^3X_4 + X_3(-X_4X_3^2 + X_4^3X_3^4X_2^2 + X_4X_3^4X_5^2 - 4X_5X_2 + 4X_4X_2^2 - 2X_4^2X_3^4X_2X_5)E_1],$$

$$m_{26} = -\sqrt{2}X_1^2X_3X_5,$$

$$m_{33} = \frac{X_1^2}{2\sqrt{2}}[3X_3^4/X_3^5 + E_1(X_3^8X_2^4X_4 + X_3^8X_5^4 - 6X_3^6X_2^2X_4^2 - 6X_3^6X_5^2 + 3X_3^4 - 8X_2^2X_3^2 + 8X_2^4X_4^2X_3^4 - 16X_2^3X_4X_5X_3^4 + 8X_2^2X_5^2X_3^4 + 16X_2^4 + 12X_3^6X_2X_4X_5 - 4X_3^8X_2^3X_4^3X_5 + 6X_3^8X_2^2X_4^2X_5^2 - 4X_3^8X_2X_4X_5^3)/X_3^5],$$

$$m_{35} = \frac{X_1^2}{2\sqrt{2}}E_1(3X_3^2X_4X_2 - 3X_3^2X_5 - X_3^4X_4^3X_3^3 + 3X_3^4X_5X_2^2X_4^2 - 3X_3^4X_5^2X_2X_4 + X_3^4X_5^3 - 4X_4X_2^3 + 4X_5X_2^2),$$

$$m_{36} = -2\sqrt{2}X_1^2X_2E_1(-X_2X_4 + X_5),$$

$$m_{44} = \frac{X_1^2}{32\sqrt{2}}[3X_3^5 + X_3(X_3^8X_2^4X_4 + X_3^8X_5^4 - 6X_3^6X_2^2X_4^2 + 12X_3^6X_2X_4X_5 - 6X_3^6X_5^2 + 3X_3^4 + 8X_2^4X_4^2X_3^4 - 8X_2^2X_3^2 - 16X_2^3X_4X_5X_3^4 + 8X_2^2X_5^2X_3^4 + 16X_2^4 - 4X_3^8X_2^3X_4^3X_5 + 6X_3^8X_2^2X_4^2X_5^2 - 4X_3^8X_2X_4X_5^3)E_1],$$

$$m_{45} = -\frac{X_1^2}{4\sqrt{2}}X_2X_3E_1(-X_3^2 + X_3^4X_2^2X_4^2 - 2X_3^4X_2X_4X_5 + X_3^4X_5^2 + 4X_2^2),$$

$$m_{46} = \frac{X_1^2}{4\sqrt{2}}[X_3^3 - X_3(-X_3^2 - 2X_3^4X_2X_4X_5 + X_3^4X_5^2 - 4X_2^2 + X_3^4X_2^2X_4^2)E_1],$$

$$m_{55} = \frac{X_1^2}{2\sqrt{2}}[X_3^3 + X_3(-X_3^2 + X_3^4X_2^2X_4^2 - 2X_3^4X_2X_4X_5 + X_3^4X_5^2 + 4X_2^2)E_1],$$

$$m_{56} = -\sqrt{2}X_1^2X_2X_3E_1,$$

$$m_{66} = \sqrt{2}X_1^2X_3(1 + E_1),$$

$$F_{11} = F_{21} = F_{36} = 0,$$

$$F_{12} = -\frac{X_1^2}{2\sqrt{2}}X_5(4X_3^2X_5^2 + 12 + 3X_3^4X_4^2)/X_3,$$

$$F_{13} = \frac{X_1^2}{\sqrt{2}}[-2X_4 + E_1(16X_5X_2^3 - 12X_2^2X_5X_2 - 2X_3^4X_4 - 3X_3^8X_4^2X_2^2X_5^2 + X_3^8X_4^2X_2X_5^3 + 16X_2^3X_5X_4^2X_3^4 - 8X_2^2X_5^2X_4X_3^4 + 3X_3^8X_4^4X_2^3X_5 - 16X_4X_2^4 + 5X_3^6X_4^2X_2^2 - X_3^8X_4^5X_2^4 + 20X_2^2X_4X_2^2 - 8X_2^4X_3^4X_4^4 - 7X_3^6X_4^2X_2X_5 + 2X_3^6X_5^2X_4)/X_3^4],$$

$$F_{14} = \frac{X_1^2}{16\sqrt{2}}[(-4X_3^4 + 3X_3^8X_4^2 + 4X_3^6X_5^2)/X_3^3 + E_1(-4X_3^4 - 6X_3^{10}X_4^4X_2^2 + 16X_3^6X_2X_4X_5 - 8X_3^6X_2^2X_2^2 - 64X_2^4 - 4X_3^{12}X_4^3X_2X_3^3 + 12X_3^{10}X_4^3X_2X_5 - 6X_3^{10}X_4^2X_5^2 + 4X_3^8X_2^4X_4^4 - 16X_3^8X_2^3X_4^3X_5 + 6X_3^{12}X_4^4X_2^2X_5^2 - 4X_3^{12}X_4^5X_2^3X_5 + 20X_3^8X_2^2X_4^2X_5^2 - 8X_3^8X_2X_4X_5^3 - 4X_3^6X_5^2 + 16X_3^4X_5^2X_2^2 + 64X_2^2X_3^2 + 3X_3^8X_4^2 - 16X_3^4X_4^2X_4^4 + X_3^{12}X_4^2X_5^4 + X_3^{12}X_4^6X_4^4)/X_3^3],$$

$$F_{15} = \frac{X_1^2}{2\sqrt{2}}[2X_3^3X_4X_5 + E_1(X_3^8X_2^2X_5^2X_2 + 8X_3^4X_4^2X_2^3 + X_3^8X_4^4X_2^3 - 3X_3^6X_4^2X_2 - 8X_3^4X_5X_2^2X_4 + 2X_3^6X_4X_5 - 2X_3^8X_4^3X_5X_2^2 - 12X_2^3X_2 + 16X_2^3)/X_3^3],$$

$$F_{16} = -\frac{X_1^2}{2\sqrt{2}}[(-X_3^6X_4^2 - 4X_3^2 - 4X_3^4X_5^2)/X_3^3 + E_1(X_3^8X_4^2X_5^2 - X_3^6X_4^2 + X_3^8X_4^4X_2^2 - 2X_3^8X_4^3X_2X_5 + 16X_2^2 - 4X_3^2 + 8X_3^4X_2^2X_4^2 - 8X_3^4X_2X_4X_5)/X_3^3],$$

$$F_{22} = [(2X_1^4X_2X_3^2X_4 - 3X_1^4X_3^2X_5)C + (-2X_1^4X_2S + 1/2X_1^4X_2X_4^2SX_3^4 - 1/2X_1^4X_4SX_5X_3^4)]\frac{E_3}{X_3} - X_1^4X_3X_5 - 2X_1^4E_2X_3X_5 + 2X_1^4E_2X_2X_3X_4,$$

$$F_{23} = [(-2X_1^4X_2X_5 + 2X_1^4X_2^2X_4)C + 4X_2^2X_1^4S/X_3^2]E_3 - 2X_1^4X_2X_5E_4 + 2X_2^2X_1^4X_4E_4,$$

$$F_{24} = (24X_1^4X_3X_2^2 + 2X_1^4X_3^5X_2X_4X_5 - X_1^4X_3^5X_5^2 + 2X_1^4X_3^3 - X_1^4X_3^5X_2^2X_4^2)CE_5/8 + (X_1^4X_3^3 - 2X_1^4X_3^5X_2^2X_4^2 + 4X_1^4X_3^5X_2X_4X_5 - 2X_1^4X_3^5X_5^2 + 8X_1^4X_3X_2^2)E_6/16 + (X_1^4X_3^3/8 + X_1^4X_3X_2^2)E_2 + X_1^4X_3^3/16,$$

$$F_{25} = -2X_1^4 E_2 X_3 X_2 - 3X_1^4 X_3 X_2 C E_5 - X_1^4 X_3 X_2 E_6 \\ - X_1^4 X_3^3 S X_2 X_4 E_5 / 2 + X_1^4 X_3^3 S X_5 E_5 / 2, \\ F_{26} = 4X_1^4 X_3 C E_5 + X_1^4 X_3 E_6 + 2X_1^4 E_2 X_3 + X_1^4 X_3,$$

$$F_{31} = \sqrt{2} X_1 X_3 (1 + E_1),$$

$$F_{32} = \frac{X_1^2}{\sqrt{2}} (X_3^3 X_4 X_5 - X_3^3 X_4^2 X_2 - 4X_2 / X_3) E_1,$$

$$F_{33} = \frac{X_1^2}{\sqrt{2}} [1 + (1 + 2X_3^2 X_2 X_4 X_5 - X_3^2 X_5^2 + 4X_2^2 / X_3^2 \\ - X_3^2 X_2^2 X_4^2) E_1],$$

$$F_{34} = \frac{X_1^2 X_2 X_3^3}{\sqrt{2}} (X_5 - X_2 X_4) E_1,$$

$$F_{35} = \frac{X_1^2 X_3^3}{\sqrt{2}} (X_2 X_4 - X_5) E_1,$$

with

$$C = \cos(X_2^2 X_4 - X_2 X_5),$$

$$S = \sin(X_2^2 X_4 - X_2 X_5),$$

$$E_1 = \exp \left[\frac{-1}{2X_3^2} (X_3^4 X_2^2 X_4^2 - 2X_3^4 X_2 X_4 X_5 + X_3^4 X_5^2 + 4X_2^2) \right],$$

$$E_2 = \exp \left[\frac{-4X_2^2}{X_3^2} \right],$$

$$E_3 = \exp \left[\frac{-1}{4X_3^2} (12X_2^2 + X_3^4 X_2^2 X_4^2 - 2X_3^4 X_2 X_4 X_5 + X_3^4 X_5^2) \right],$$

$$E_4 = \exp \left[\frac{1}{X_3^2} (-4X_2^2 - X_3^4 X_2^2 X_4^2 + 2X_3^4 X_2 X_4 X_5 - X_3^4 X_5^2) \right],$$

$$E_5 = \exp \left[\frac{-4X_2^2}{X_3^2} - \frac{-1}{4X_3^2} (X_3^4 X_2^2 X_4^2 - 2X_3^4 X_2 X_4 X_5 \\ + X_3^4 X_5^2 - 4X_2^2) \right],$$

$$E_6 = \exp \left[\frac{-4X_2^2}{X_3^2} - X_3^2 X_2^2 X_4^2 + 2X_3^2 X_2 X_4 X_5 - X_3^2 X_5^2 \right].$$

-
- [1] G. P. Agrawal, *Nonlinear Fiber Optics*, 2nd ed. (Academic, New York, 1995).
- [2] A. Hasegawa and Y. Kodama, *Solitons in Optical Communication* (Oxford University Press, New York, 1995).
- [3] V. E. Zakharov and S. Wabnitz, *Optical Solitons: Theoretical Challenges and Industrial Perspectives* (Springer-Verlag, Berlin, 1998).
- [4] D. K. Campbell, M. Peyrard, and P. Sodano, *Physica D* **19**, 165 (1986).
- [5] C. R. Willis, M. El-Batanouny, and P. Stancioff, *Phys. Rev. B* **33**, 1904 (1986).
- [6] R. Boesch, P. Stancioff, and C. R. Willis, *Phys. Rev. B* **38**, 6713 (1988).
- [7] R. Boesch and C. R. Willis, *Phys. Rev. B* **39**, 361 (1989).
- [8] R. Boesch, C. R. Willis, and M. El-Batanouny, *Phys. Rev. B* **40**, 2284 (1989).
- [9] C. R. Willis and R. Boesch, *Phys. Rev. B* **41**, 4570 (1990).
- [10] P. Tchofo Dinda, R. Boesch, E. Coquet, and C. R. Willis, *Phys. Rev. B* **46**, 3311 (1992).
- [11] P. Tchofo Dinda and C. R. Willis, *Phys. Rev. E* **51**, 4958 (1995).
- [12] P. A. M. Dirac, *Lectures on Quantum Mechanics* (Academic, New York, 1964).
- [13] R. Boesch and M. Peyrard, *Phys. Rev. B* **43**, 8491 (1991).
- [14] R. Boesch and C. R. Willis, *Phys. Rev. B* **42**, 6371 (1990).
- [15] V. E. Zakharov and A. B. Shabat, *Zh. Éksp. Teor. Fiz.* **61**, 118 (1971) [*Sov. Phys. JETP* **34**, 62 (1972)].
- [16] A. Hasegawa and F. Tappert, *Appl. Phys. Lett.* **23**, 142 (1973).
- [17] L. F. Mollenauer, R. H. Stolen, and J. P. Gordon, *Phys. Rev. Lett.* **45**, 1095 (1980).
- [18] L. A. Ostrovskii, *Sov. Phys. Tech. Phys.* **8**, 679 (1964).
- [19] V. I. Bespalov and V. I. Talanov, *Pis'ma Zh. Éksp. Teor. Fiz.* **3**, 471 (1966) [*JETP Lett.* **3**, 307 (1966)].
- [20] J. P. Gordon, *Opt. Lett.* **11**, 662 (1986).
- [21] D. J. Kaup and A. C. Newell, *Proc. R. Soc. London, Ser. A* **361**, 413 (1978).
- [22] V. I. Karpman and E. M. Maslov, *Zh. Éksp. Teor. Fiz.* **73**, 537 (1977) [*Sov. Phys. JETP* **46**, 281 (1977)].
- [23] V. I. Karpman and V. V. Solovév, *Physica D* **3**, 487 (1981).
- [24] A. Bonderson, M. Lisak, and D. Anderson, *Phys. Scr.* **20**, 479 (1979).
- [25] J. G. Caputo, N. Flytzanis, and M. P. Sorensen, *J. Opt. Soc. Am. B* **12**, 139 (1995).
- [26] S. Wabnitz, Y. Kodama, and A. B. Aceves, *Opt. Fiber Technol.: Mater., Devices Syst.* **1**, 187 (1995).
- [27] W. L. Kath and N. F. Smyth, *Phys. Rev. E* **51**, 1484 (1995).
- [28] L. F. Mollenauer, S. G. Evangelides, and J. P. Gordon, *J. Lightwave Technol.* **9**, 1991 (1991).
- [29] D. Anderson, *Phys. Rev. A* **27**, 3135 (1983).
- [30] I. Gabitov and S. K. Turitsyn, *Opt. Lett.* **21**, 327 (1996).
- [31] S. K. Turitsyn, I. Gabitov, E. W. Laedke, V. K. Mezentsev, S. L. Musher, E. G. Shapiro, T. Schäfer, and K. H. Spatschek, *Opt. Commun.* **151**, 117 (1998).
- [32] T. Georges, *J. Opt. Soc. Am. B* **15**, 1553 (1998).
- [33] H. Sugahara, A. Maruta, and Y. Kodama, *Opt. Lett.* **24**, 145 (1999).

- [34] T. Hirooka and A. Hasegawa, *Opt. Lett.* **23**, 768 (1998).
- [35] M. Wald, B. A. Malomed, and F. Lederer, *Opt. Commun.* **172**, 31 (1999).
- [36] S. Wabnitz and F. Neddham, *Opt. Commun.* **183**, 395 (2000).
- [37] T. S. Yang and W. L. Kath, *Physica D* **149**, 80 (2001).
- [38] A. Berntson, D. Anderson, M. Lisak, M. L. Quiroga-Teixeiro, and M. Karlson, *Opt. Commun.* **15**, 153 (1996).
- [39] T. I. Lakoba, J. Yang, D. J. Kaup, and B. A. Malomed, *Opt. Commun.* **149**, 366 (1998).
- [40] C. Pare and P. A. Belanger, *Opt. Lett.* **25**, 881 (2000).
- [41] F. M. Knox, W. Forysiak, and N. J. Doran, *J. Lightwave Technol.* **13**, 1955 (1995).
- [42] F. Kh. Abdullaev and J. G. Caputo, *Phys. Rev. E* **58**, 6637 (1998).
- [43] P. Tchofo Dinda, A. B. Moubissi, and K. Nakkeeran, *J. Phys. A* **34**, L103 (2001).
- [44] T. I. Lakoba and D. J. Kaup, *Phys. Rev. E* **58**, 6728 (1998).
- [45] S. K. Turitsyn, T. Schäfer, K. H. Spatschek, and V. K. Mezentsev, *Opt. Commun.* **163**, 122 (1999).
- [46] P. Tchofo Dinda, K. Nakkeeran, and A. B. Moubissi, *Opt. Commun.* **187**, 427 (2001).
- [47] A. V. Mikhailov, in Ref. [3], p. 68.
- [48] A. Ralston, *A First Course in Numerical Analysis* (McGraw-Hill, New York, 1965).
- [49] S. Kumar, M. Wald, F. Lederer, and A. Hasegawa, *Opt. Lett.* **23**, 1019 (1998).
- [50] H. Sugahara, H. Kato, and Y. Kodama, *Electron. Lett.* **34**, 902 (1998).
- [51] W. Forysiak, J. L. F. Devaney, N. J. Smith, and N. J. Doran, *Opt. Lett.* **22**, 600 (1997).
- [52] J. L. F. Devaney, W. Forysiak, A. M. Niculae, N. J. Smith, and N. J. Doran, *Opt. Lett.* **22**, 1695 (1997).
- [53] E. A. Golovchenko, A. N. Pilipetskii, and C. R. Menyuk, *Opt. Lett.* **22**, 1156 (1997).
- [54] E. Pincemin, F. Neddham, and O. Leclerc, *Opt. Lett.* **25**, 2000 (2000).
- [55] M. J. Ablowitz, G. Biondini, S. Chakravarty, and R. L. Horne, *Opt. Commun.* **150**, 305 (1998).
- [56] D. J. Kaup, B. A. Malomed, and J. Yang, *Opt. Lett.* **23**, 1600 (1998).
- [57] N. K. Cheung, K. Nosu, and G. Winzer, special issue on dense wavelength division multiplexing, *IEEE J. Sel. Areas Commun.* **8** (1990).
- [58] C. A. Brackett, *IEEE J. Sel. Areas Commun.* **8**, 948 (1990).